Electronic Supplementary Material (ESI) for RSC Advances.

Supplementary Information

Reinvestigation of Passerini and Ugi scaffolds as multistep apoptotic inducers *via* dual modulation of caspase 3/7 and p53-MDM2 signaling for halting breast cancer

Mohammed Salah Ayoup [a,*], Yasmin Wahby [a], Hamida Abdel-Hamid [a], Marwa M. Abu-Serie [b], Sherif Ramadan[c,d], Assem Barakat [e,*], Mohamed Teleb [f] and Magda M. F. Ismail[g]

[a]Chemistry Department, Faculty of Science, Alexandria University, P.O. Box 426, Alexandria, 21321, Egypt
[b]Medical Biotechnology Department, Genetic Engineering and Biotechnology Research Institute, City of Scientific Research and Technological Applications (SRTA-City), Egypt
[c]Chemistry Department, Michigan State University, East Lansing, MI 48824, USA.).
[d]Department of Chemistry, Benha University, Benha, Egypt.
[e]Department of Chemistry, College of Science, King Saud University, P.O. Box 2455, Riyadh 11451, Saudi Arabia;
[f]*Department of Pharmaceutical Chemistry, Faculty of Pharmacy, Alexandria University, Alexandria, 21521, Egypt*
[g]Department of pharmaceutical Medicinal Chemistry, Faculty of Pharmacy (Girls), Al–Azhar University, Cairo, 11754, Egypt.
*****Correspondence: mohammedsalahayoup@gmail.com & Mohamed.salah@alexu.edu.eg; ambarakat@ksu.edu.sa; Tel.: +966-11467-5992; +966-11467-5901 A.B.)

Contents **Page**

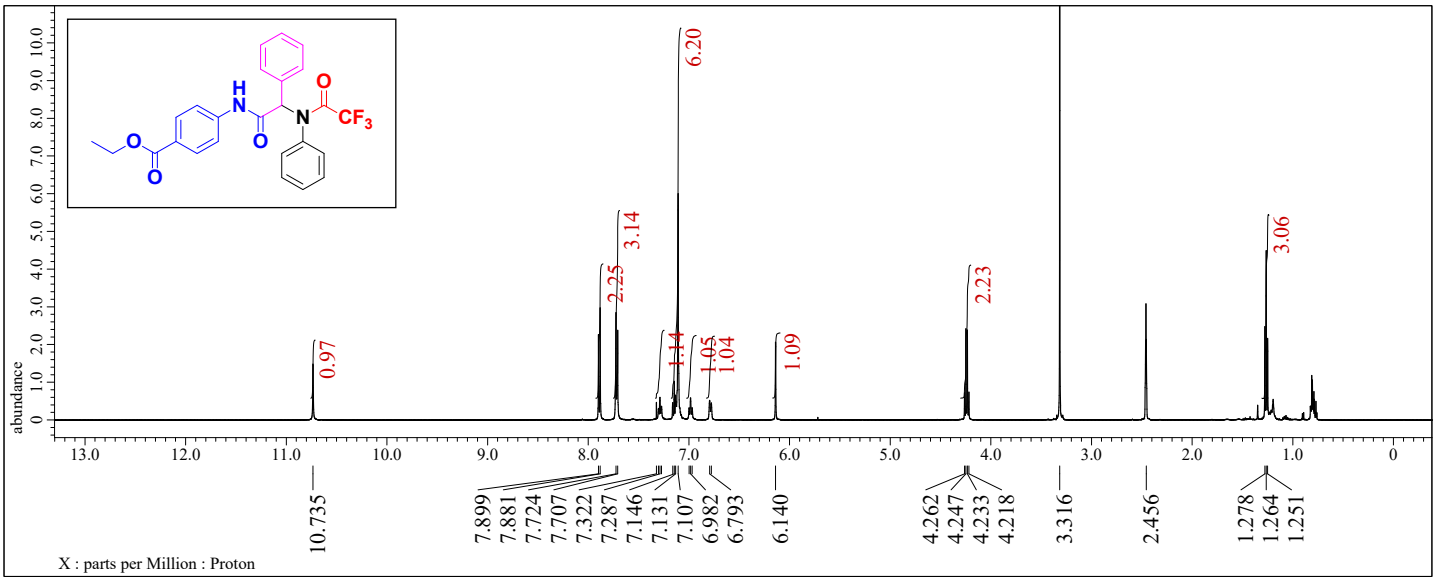

Figure S1. ^{1}H-NMR (DMSO-*d6*) of **2**

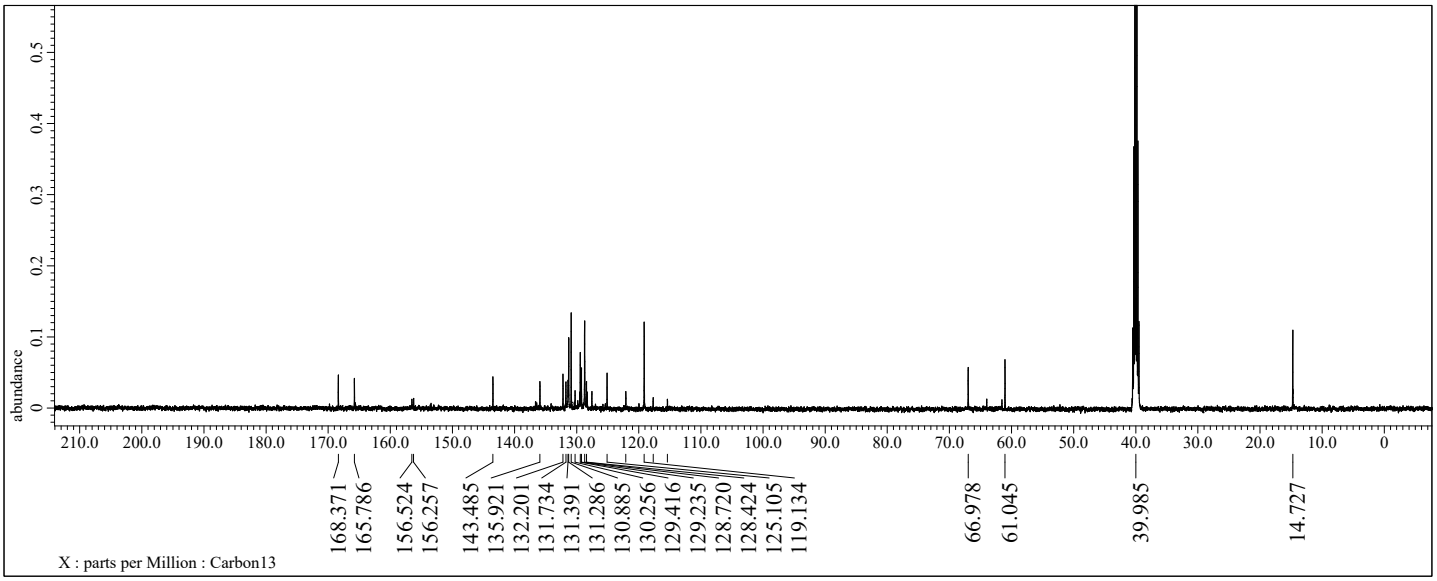

Figure S2. ^{13}C-NMR (DMSO-d_6) of **2**

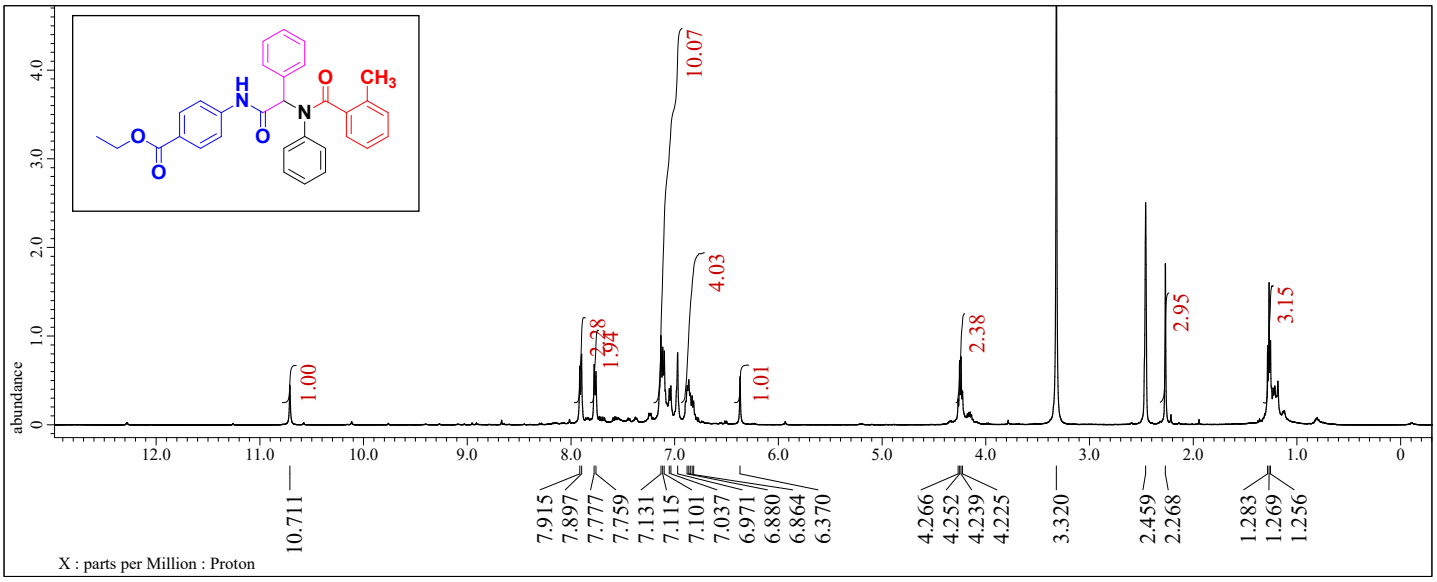

Figure S3. ^{1}H-NMR (DMSO- d_6) of **3**

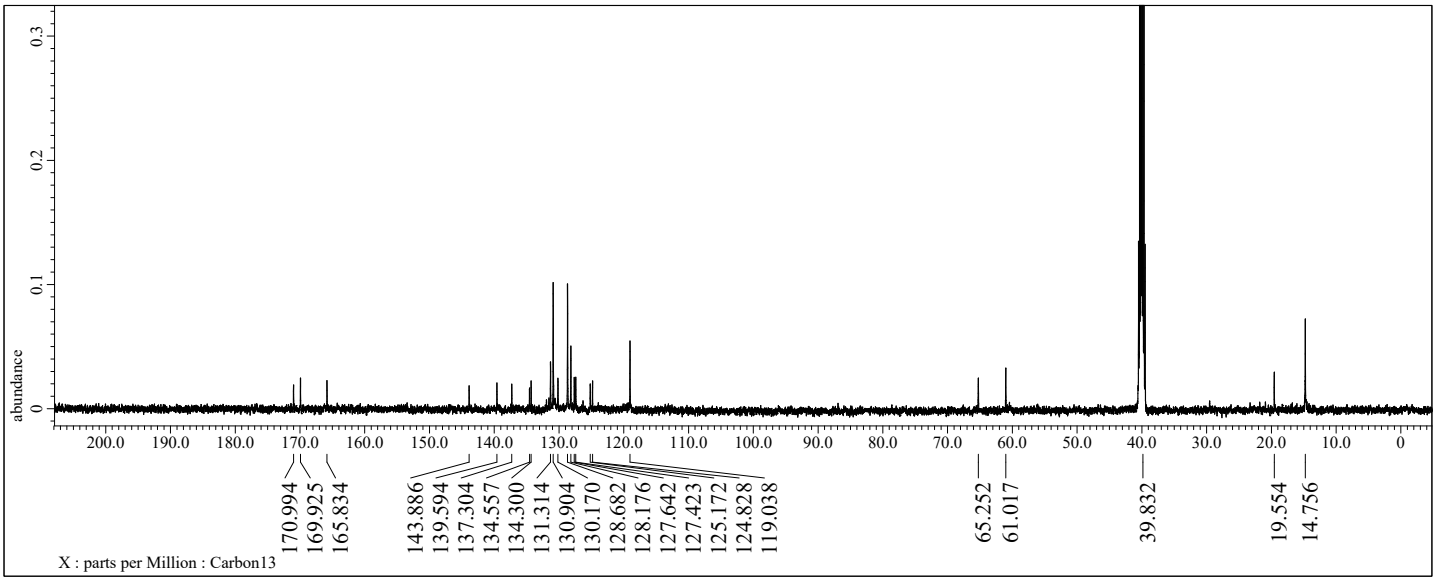

Figure S4. ^{13}C-NMR (DMSO- d_6) of **3**

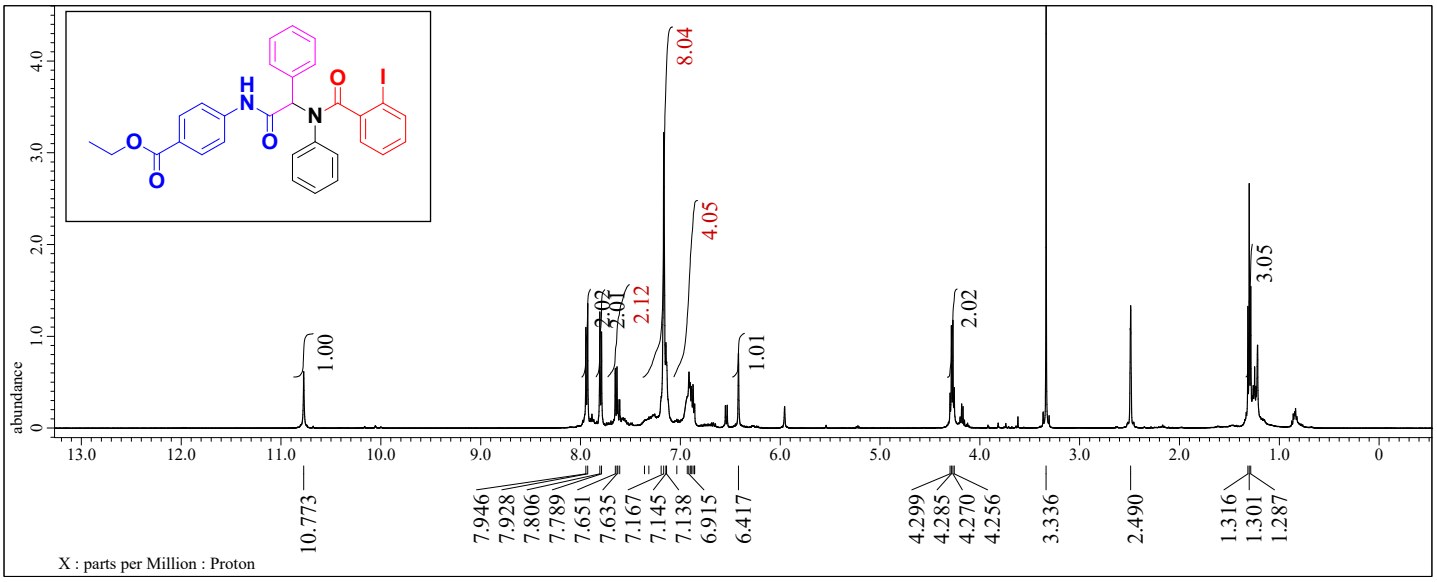

Figure S5. ^{1}H-NMR (DMSO- d_6) of **4**

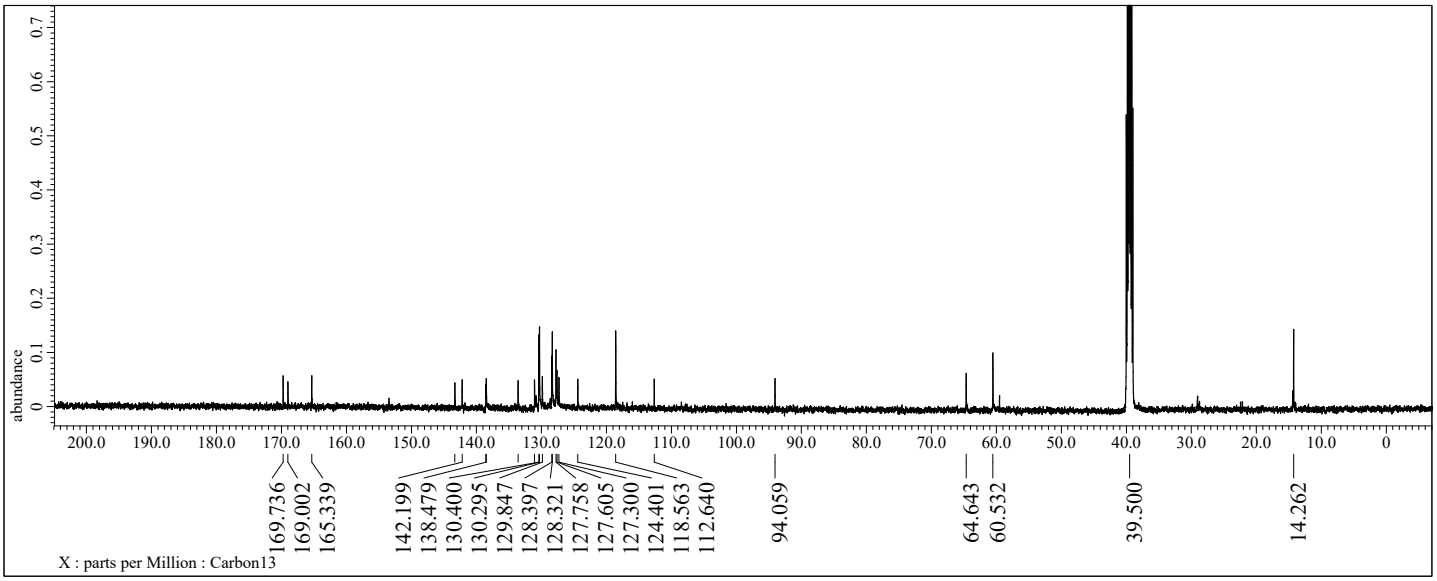

Figure S6. ^{13}C-NMR (DMSO- d_6) of **4**

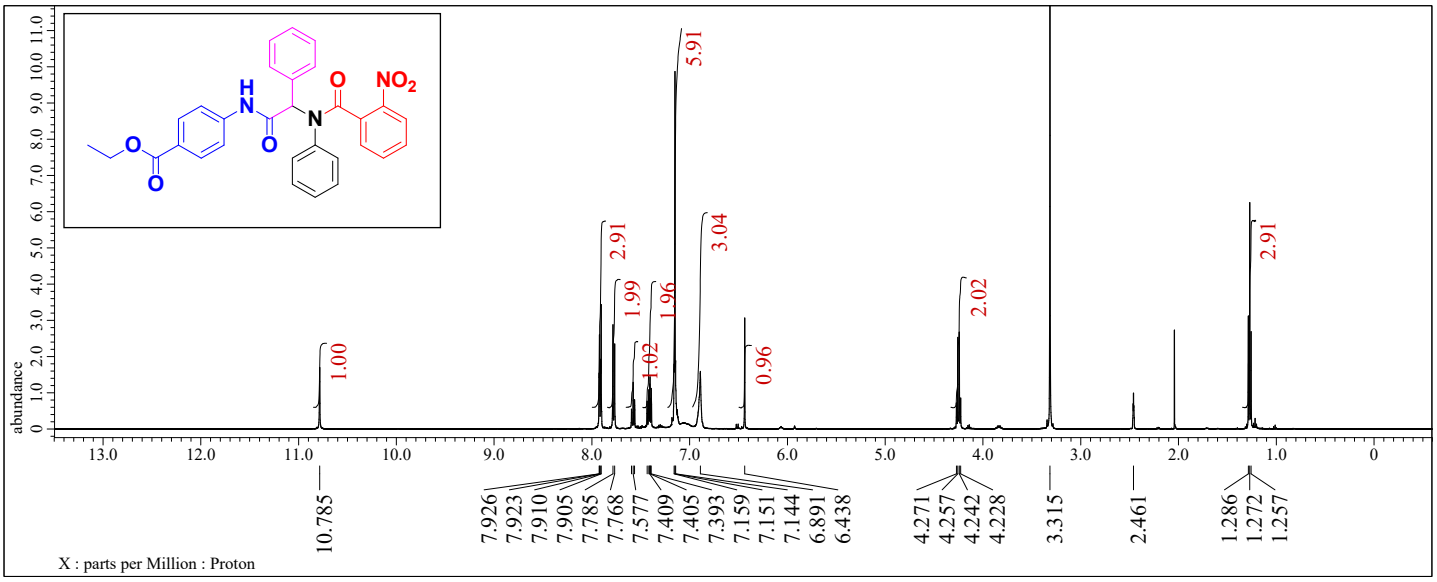

Figure S7. ^{1}H-NMR (DMSO- d_6) of **5**

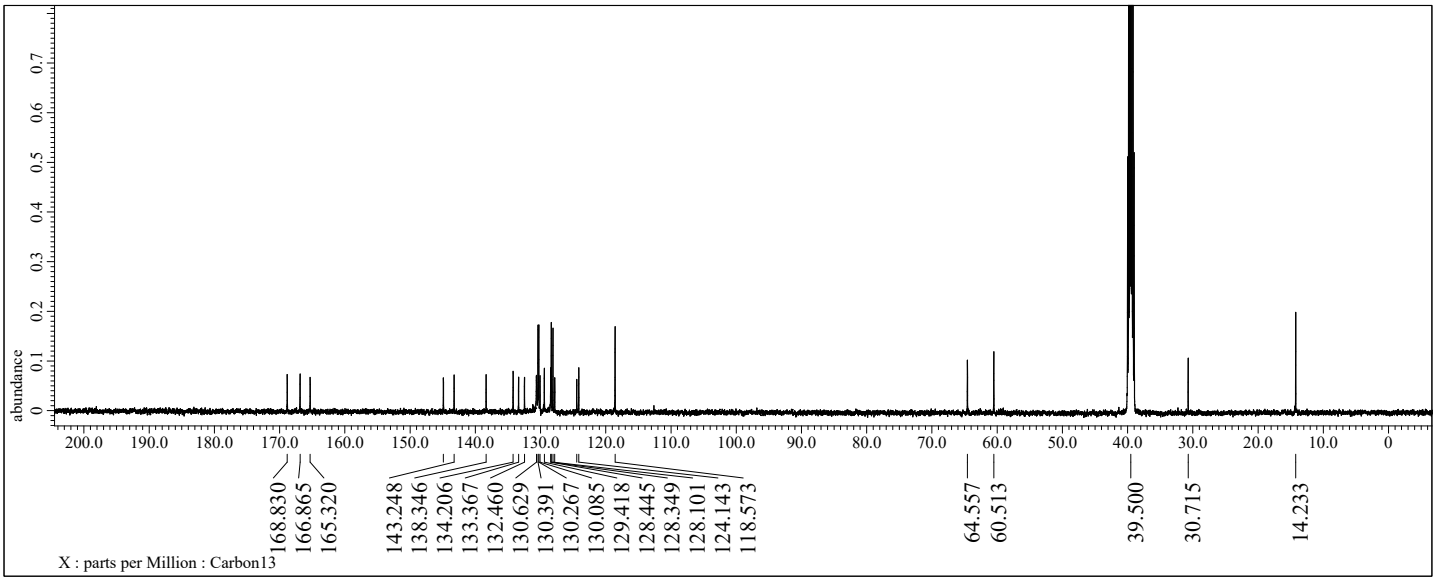

Figure S8. ^{13}C-NMR (DMSO- d_6) of **5**

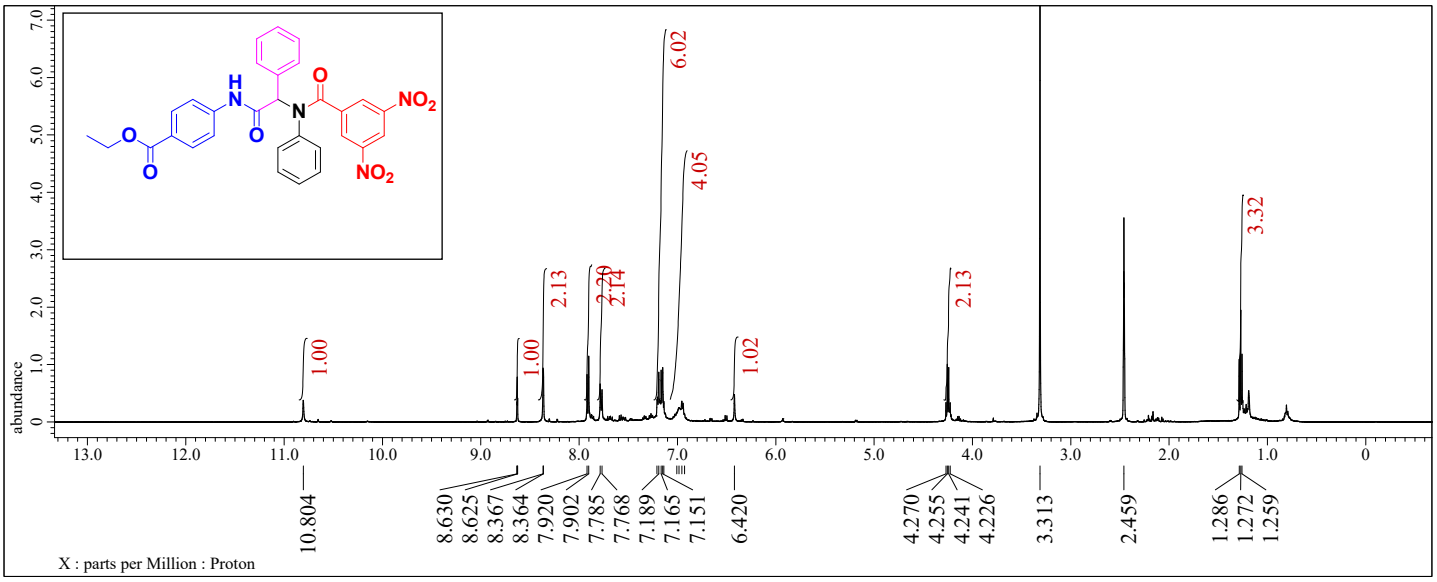

Figure S9. ^{1}H-NMR (DMSO- d_6) of **6**

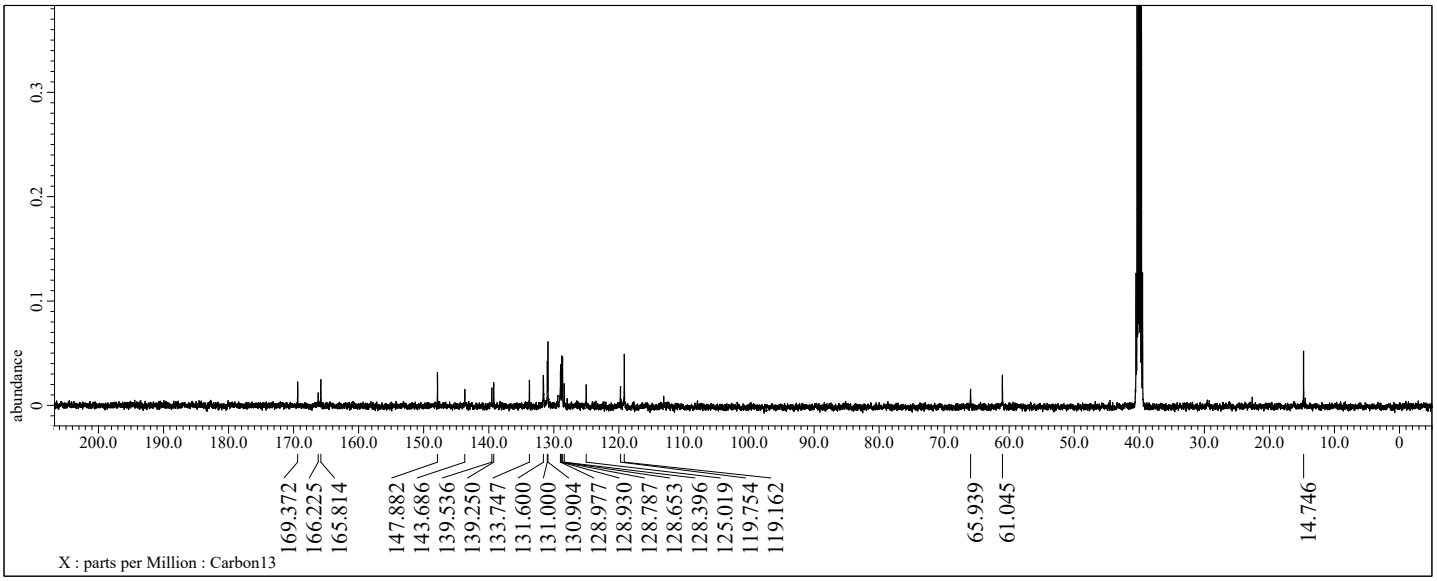

Figure S10. ^{13}C-NMR (DMSO- d_6) of **6**

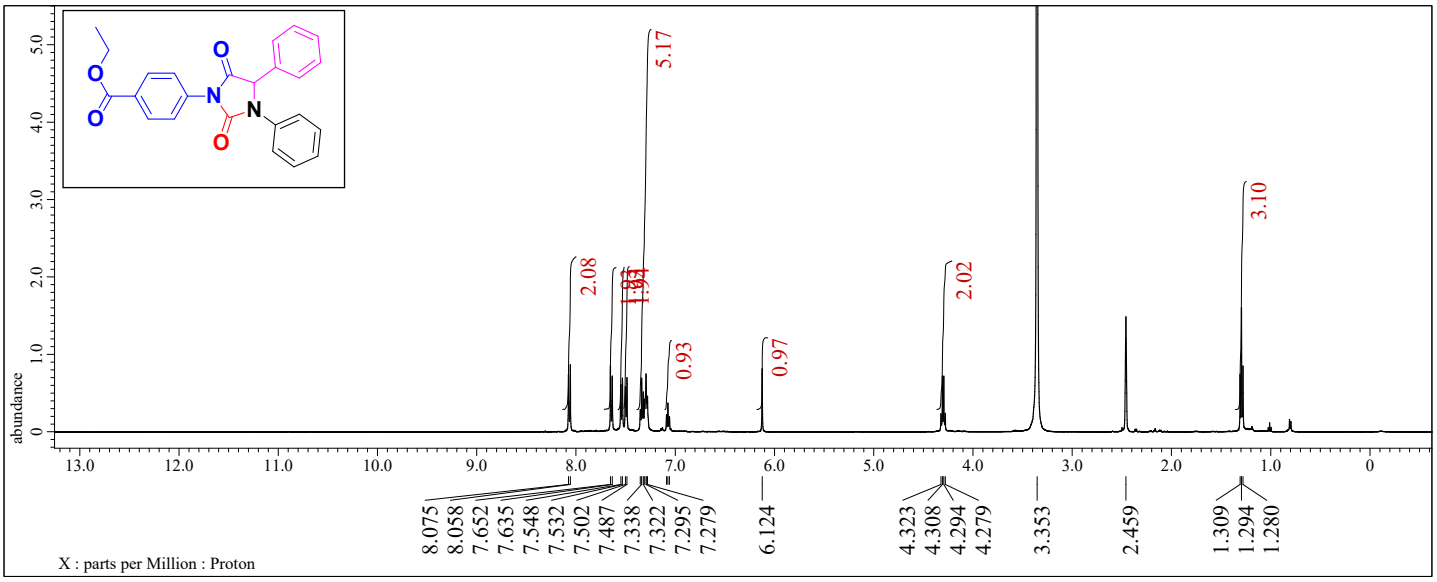

Figure S11. ^{1}H-NMR (DMSO- d_6) of **8**

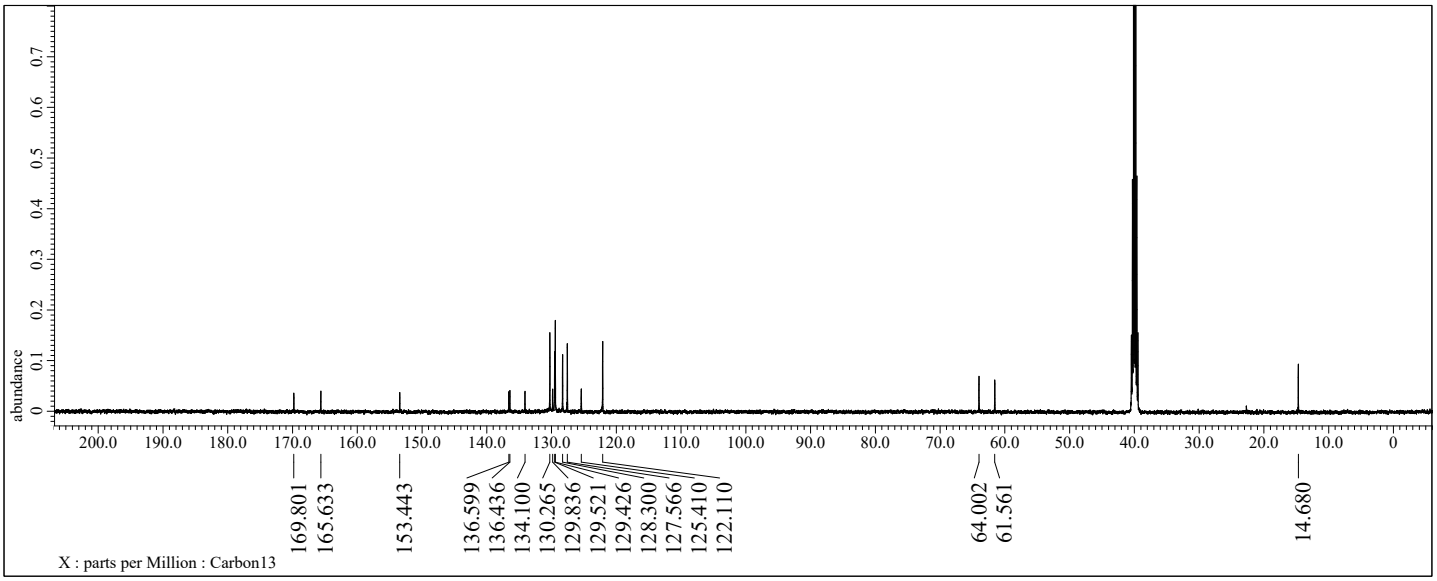

Figure S12. ^{13}C-NMR (DMSO- d_6) of **8**

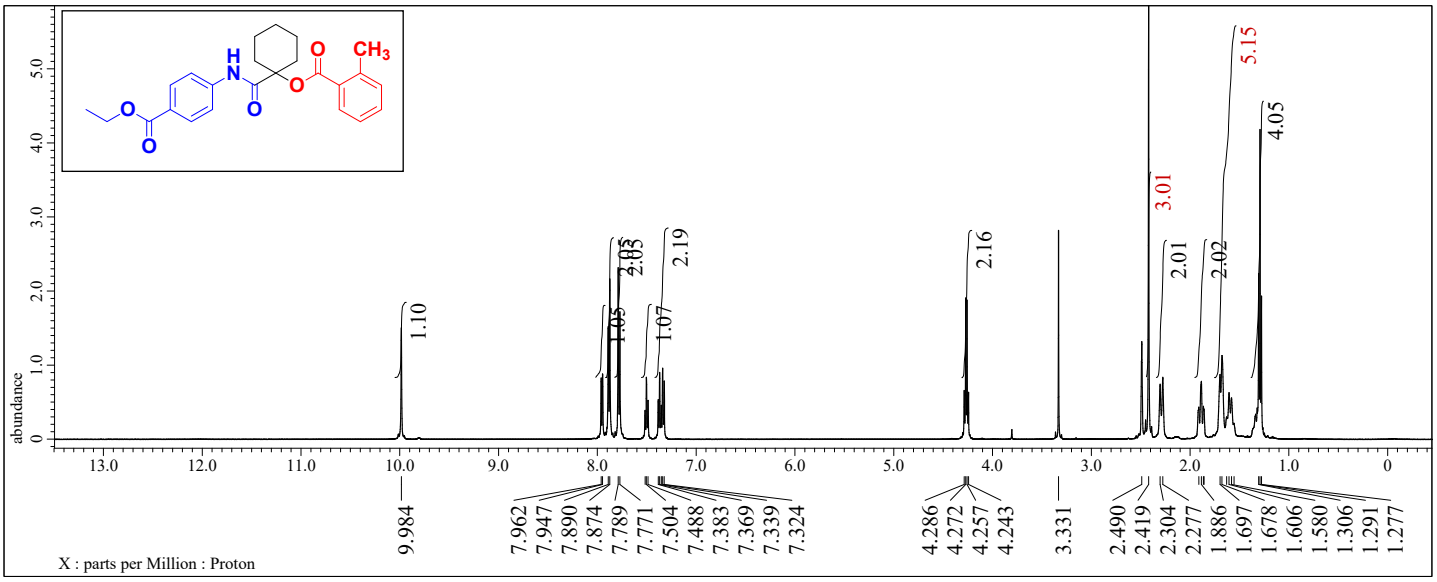

Figure S13. ^{1}H-NMR (DMSO- d_6) of **9**

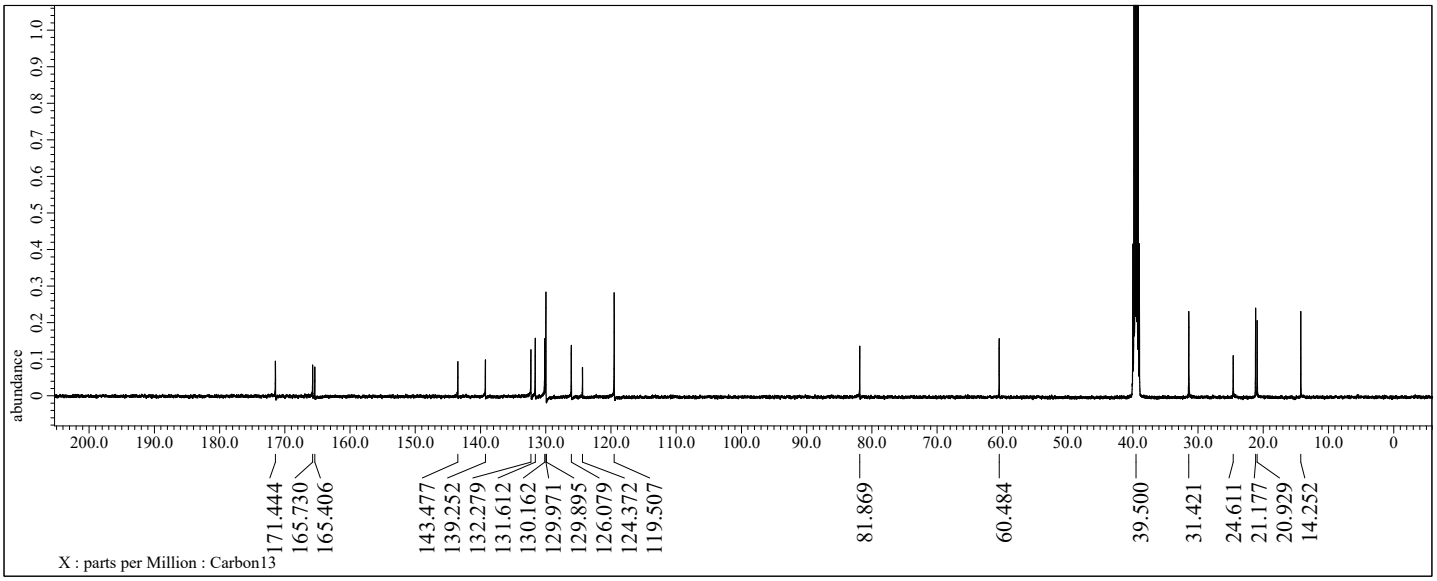

Figure S14. ^{13}C-NMR (DMSO- d_6) of **9**

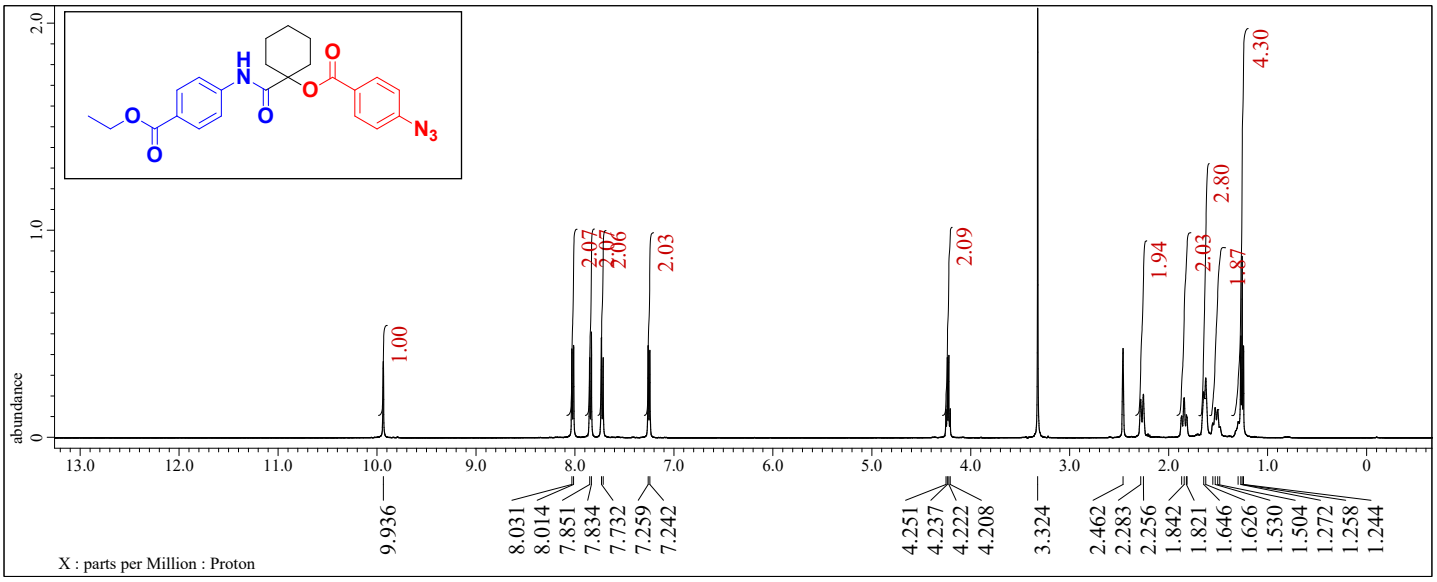

Figure S15. ^{1}H-NMR (DMSO- d_6) of **10**

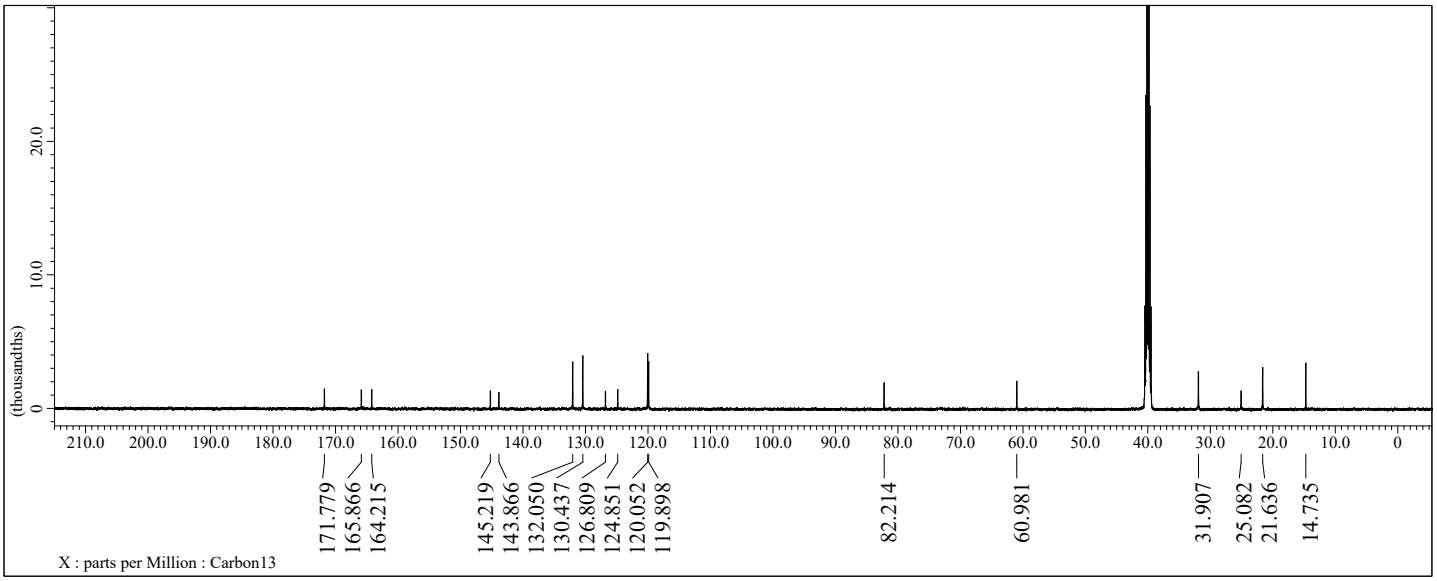

Figure S16. ^{13}C-NMR (DMSO- d_6) of **10**

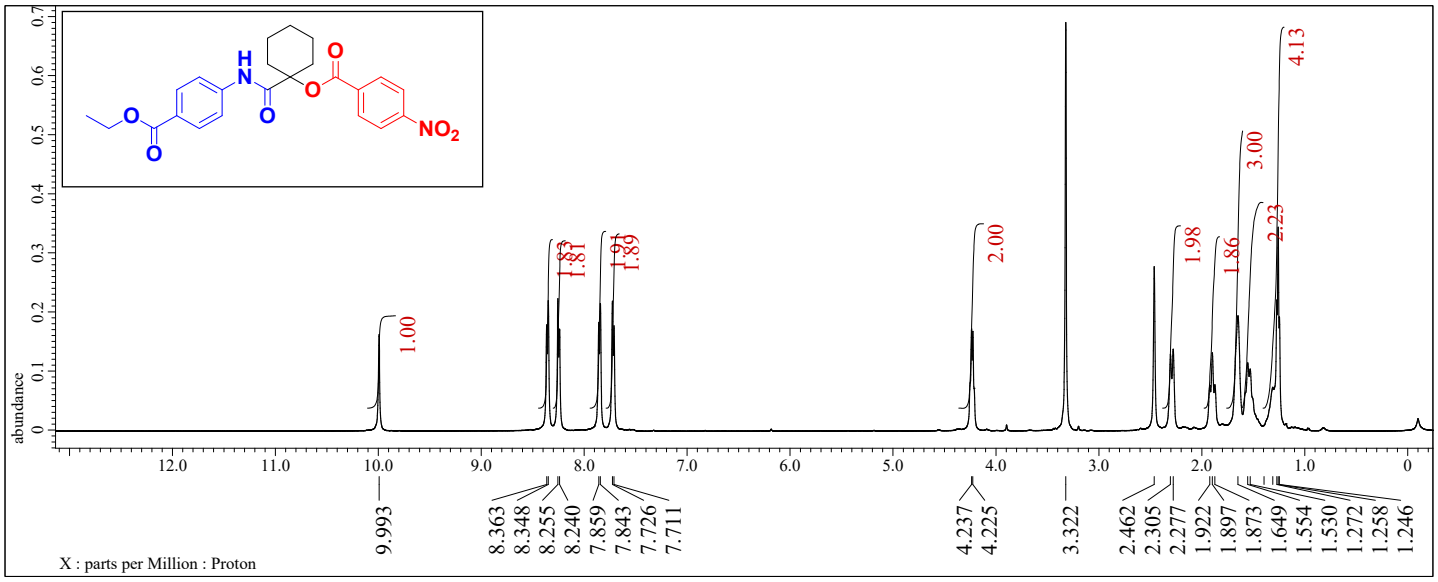

Figure S17. ^{1}H-NMR (DMSO- d_6) of **11**

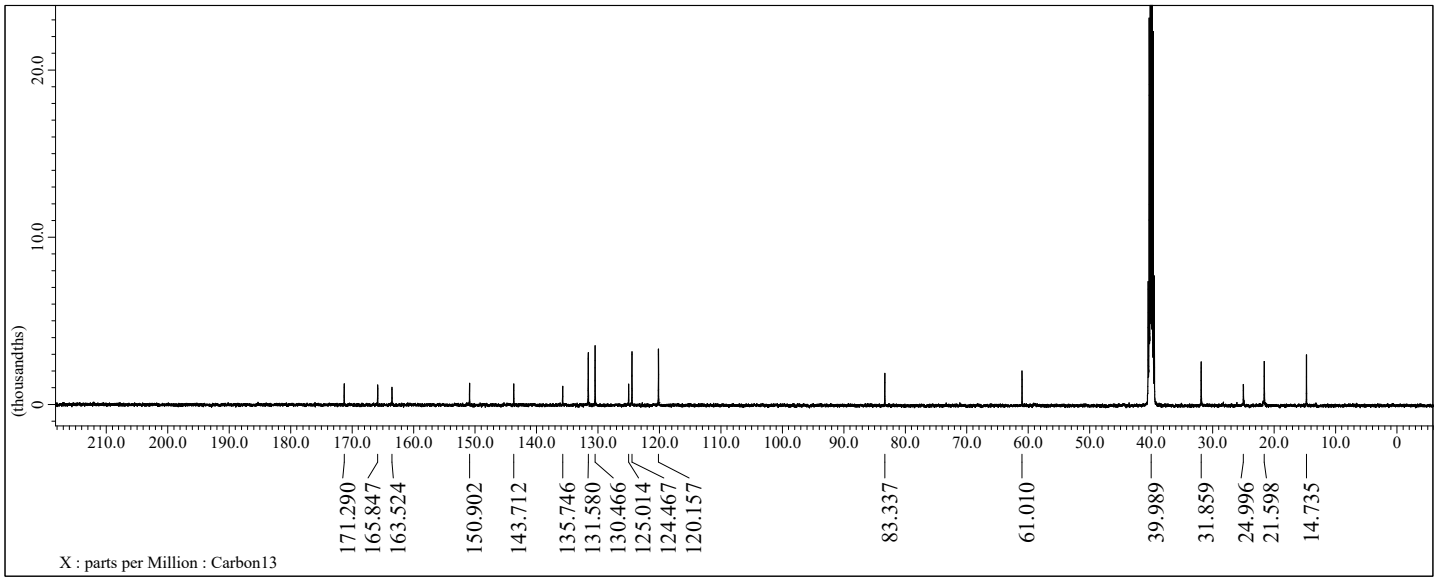

Figure S18. ^{13}C-NMR (DMSO- d_6) of **11**

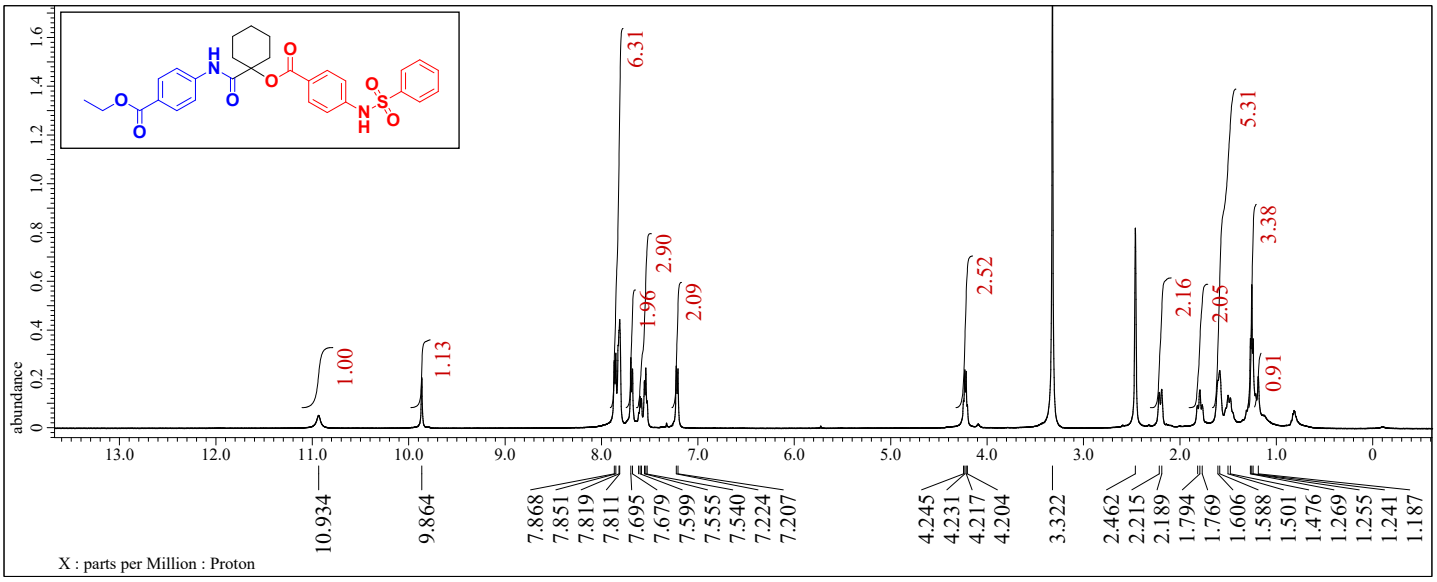

Figure S19. ^{1}H-NMR (DMSO- d_6) of **12**

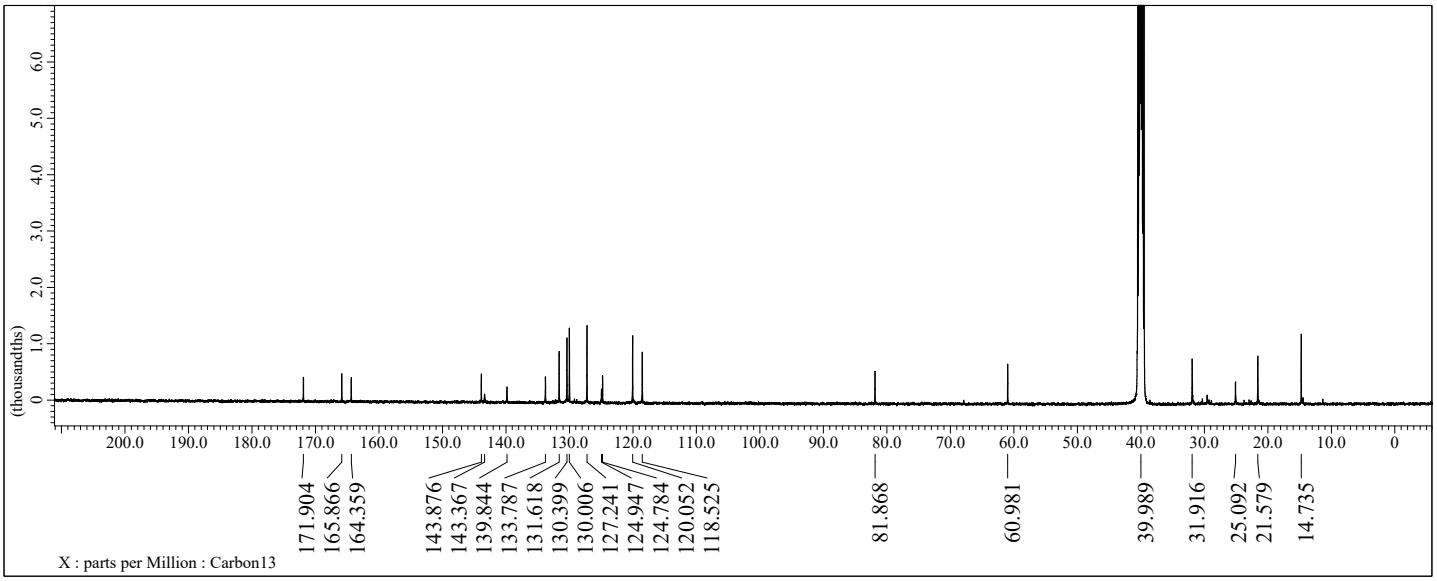

Figure S20. ^{13}C-NMR (DMSO- d_6) of **12**

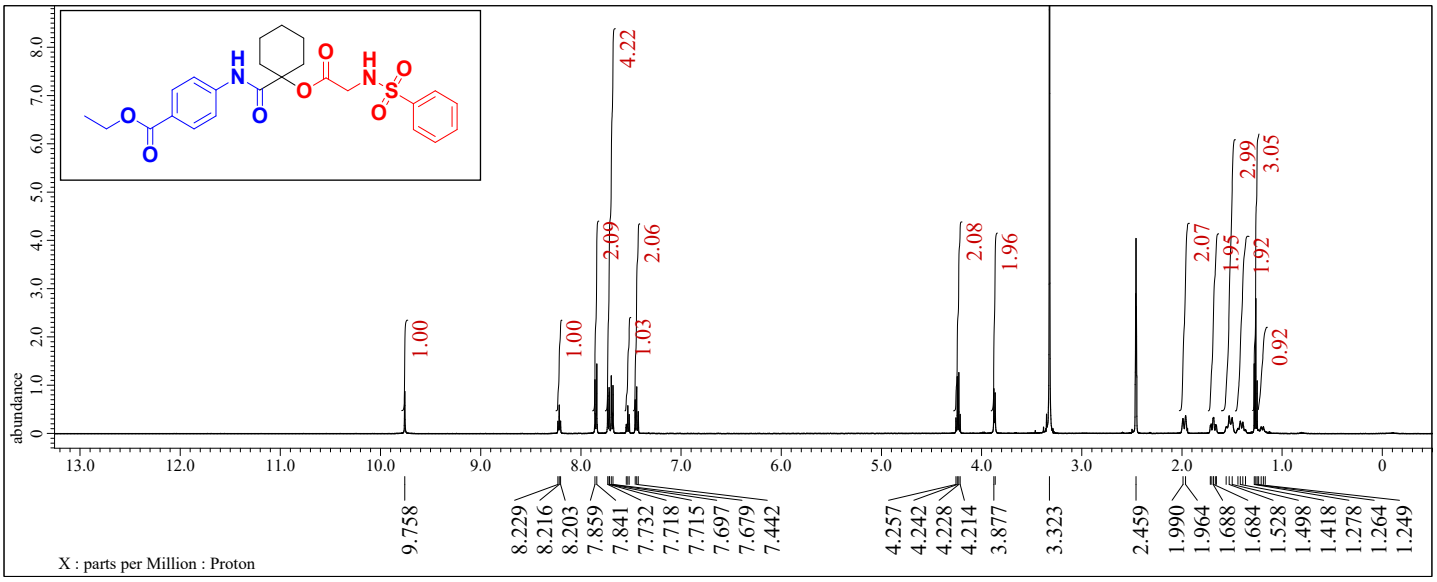

Figure S21. ^{1}H-NMR (DMSO- d_6) of **13**

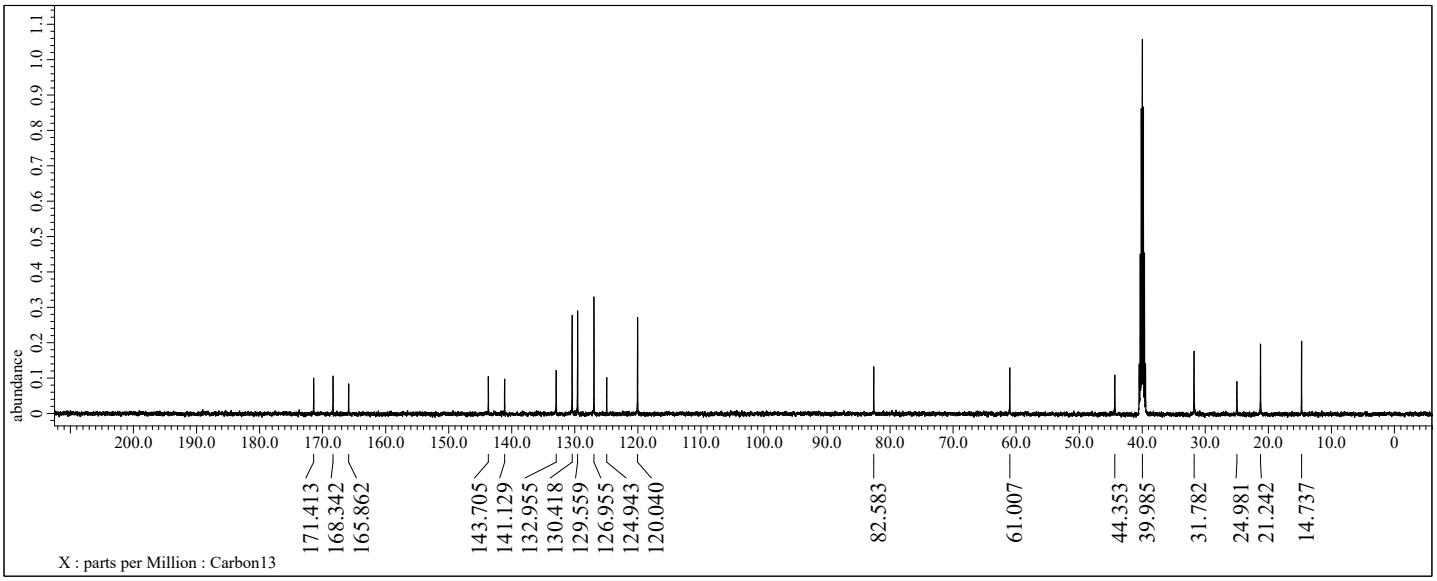

Figure S22. ^{13}C-NMR (DMSO- d_6) of **13**

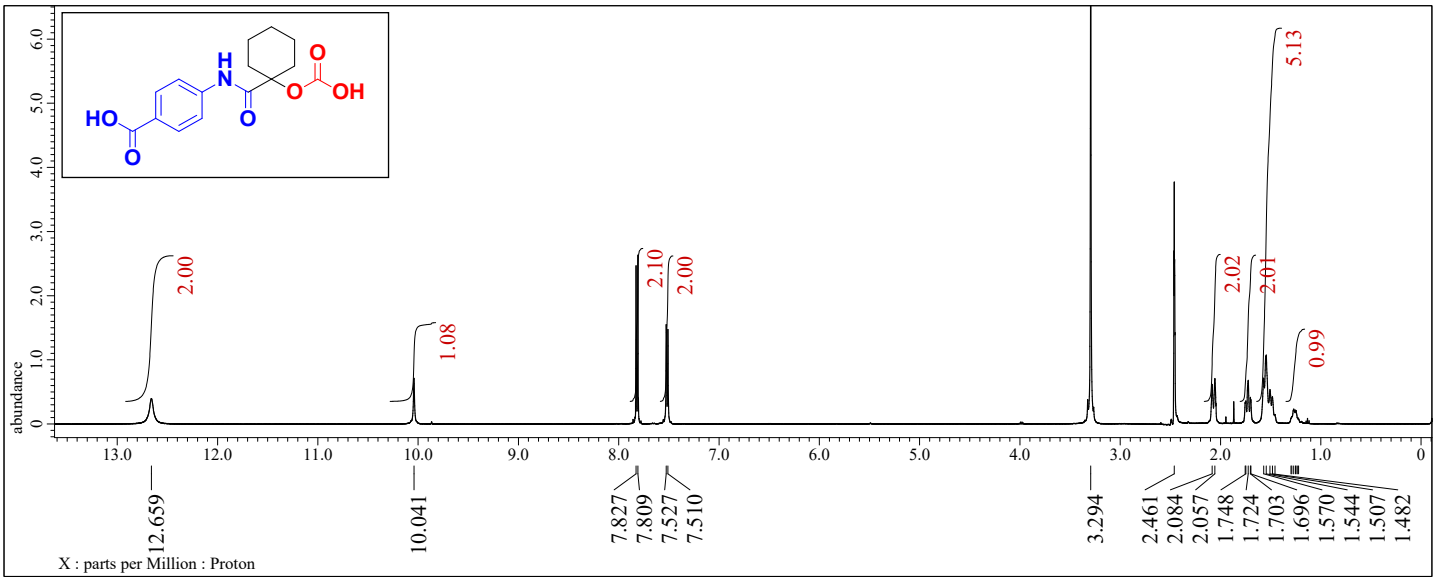

Figure S23. ^{1}H-NMR (DMSO-*d6*) of **15**

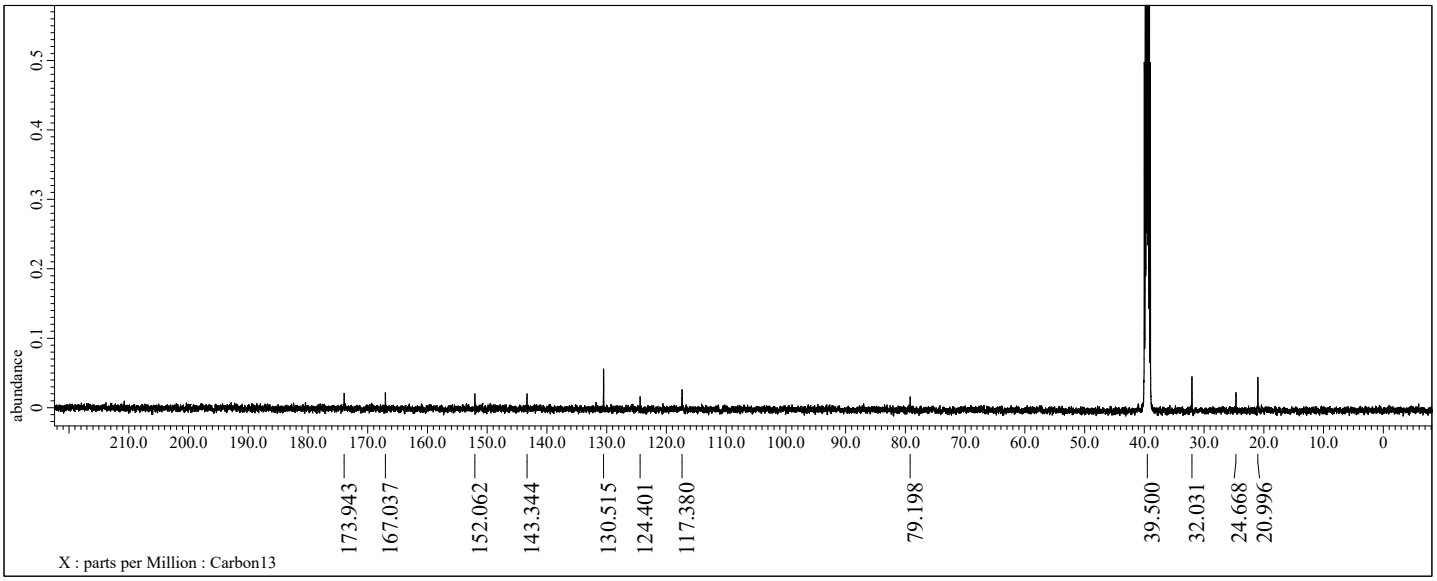

Figure S24. ^{13}C-NMR (DMSO- d_6) of **15**

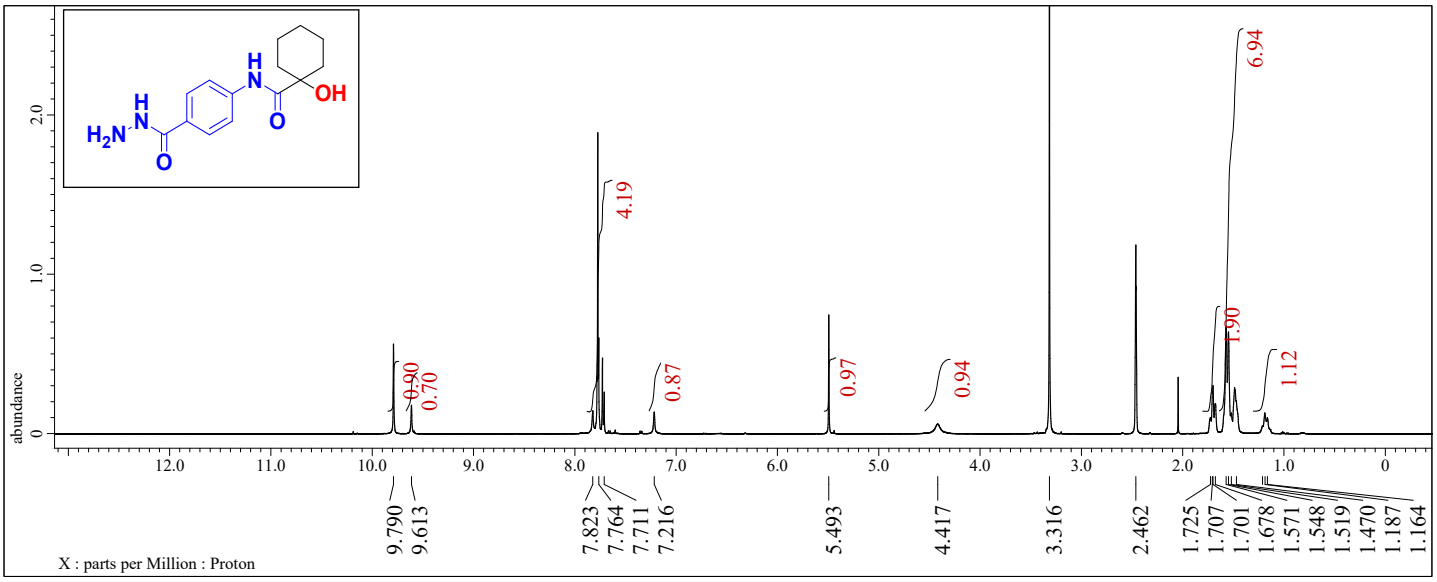

Figure S25. ^{1}H-NMR (DMSO- d_6) of **16**

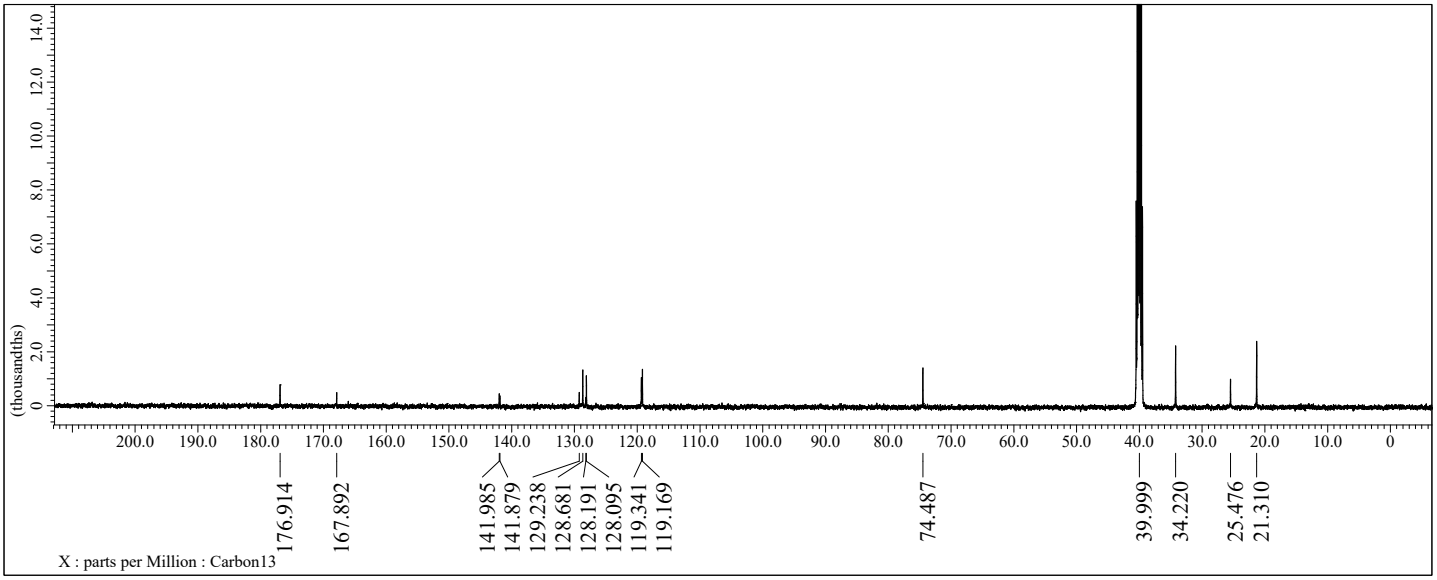

Figure S26. ^{13}C-NMR (DMSO- d_6) of **16**

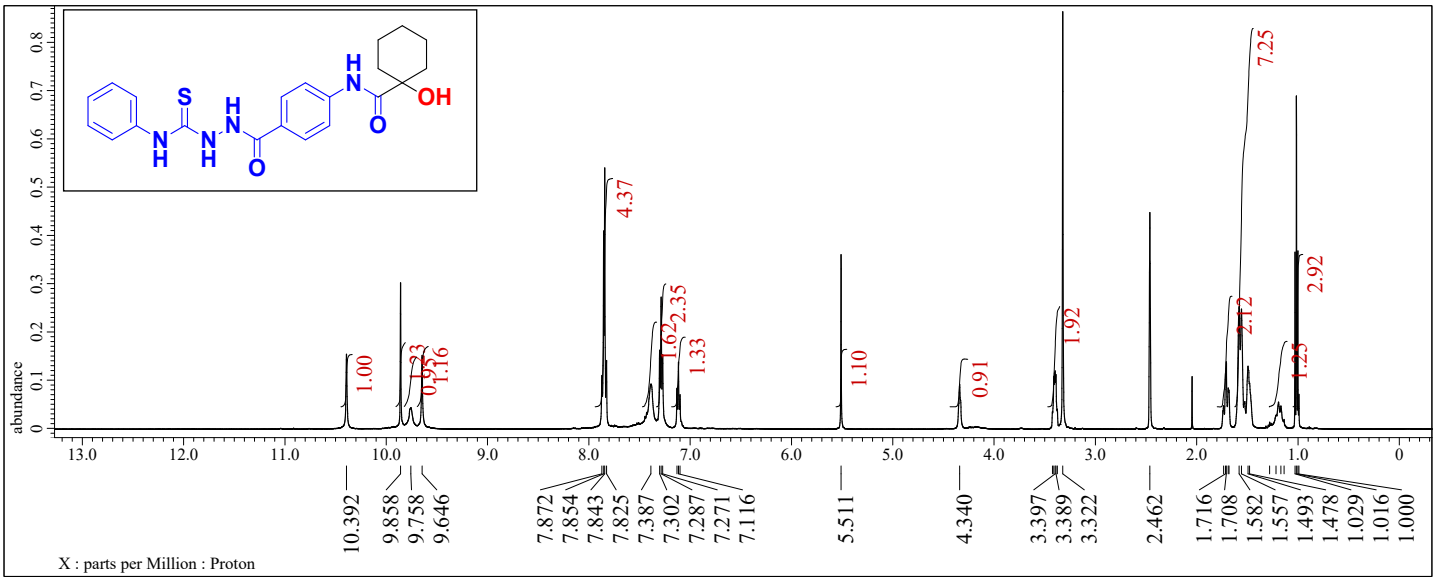

Figure S27. ^{1}H-NMR (DMSO- d_6) of **17**

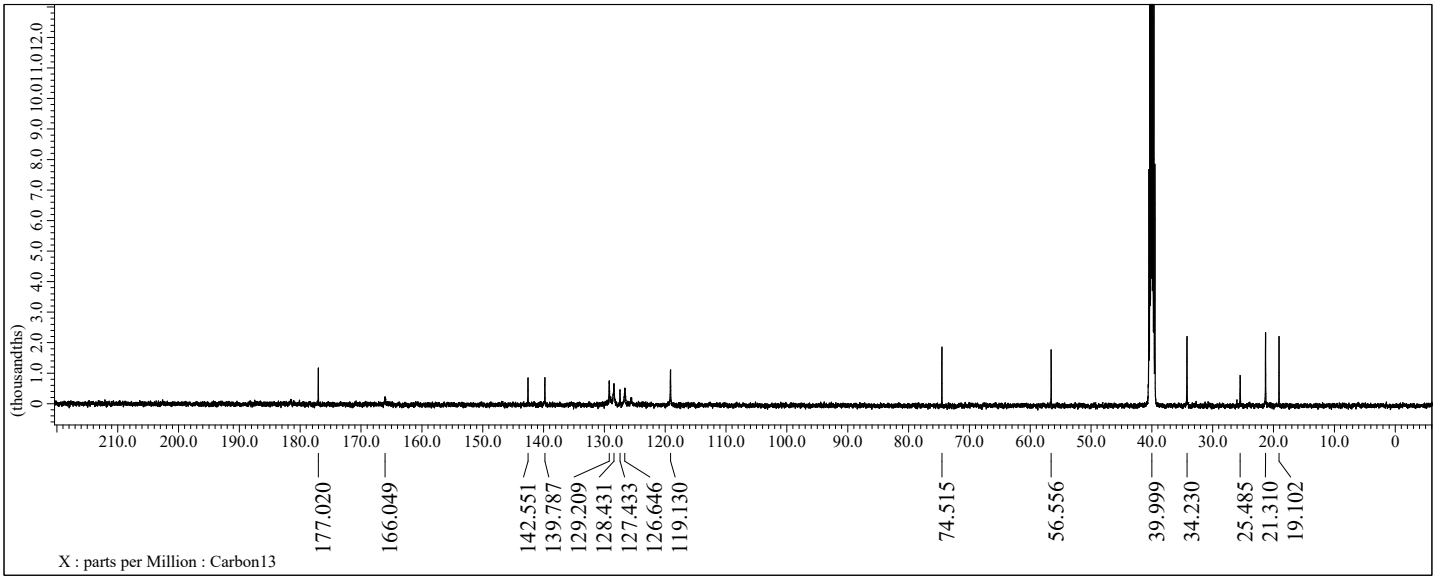

Figure S28. ^{13}C-NMR (DMSO- d_6) of **17**

2. Materials and Equipment.

Commercially available reagents and solvents were purified according to standard procedures. Dried glassware was used for all reactions. ^{1}H-NMR data were recorded by JEOLJNM ECA 500 MHz. The deuterated solvent was used as an internal deuterium lock. ^{13}C-NMR data were recorded using 125 MHz UDEFT pulse sequence and broad-band proton decoupling. Coupling constants were recorded in Hertz (J/Hz). Internal reference for NMR spectra is tetramethylsilane at 0.00 ppm. IR [ν/cm^{-1}] data were recorded using Perkin Elmer; FT-IR Spectrum BX and Bruker tensor 37 FT-IR. Melting points were measured by Thermo Scientific, Model NO. 1002D; 220-240v; 200W; 50/60Hz and were uncorrected. Thin layer chromatography (TLC) was performed on silica gel plastic plates and the spots were indicated and visualized using UV VILBER LOURMAT 4w-265nm or 254 nm tube.

3. Biological evaluation

3.1. Determination of cytotoxicity

Normal human cell line:

Normal human lung fibroblast Wi-38 cell line was used to detect cytotoxicity of the studied compounds. Wi-38 cell line was cultured in DMEM medium-contained 10% fetal bovine serum (FBS), seeded as 5x10^{3} cells per well in 96-well cell culture plate and incubated at 37ºC in 5% CO_2 incubator. After 24 h for cell attachment, serial concentrations of the synthetic compounds were incubated with Wi-38 cells for 72 h. Cell viability was assayed by MTT method (Mosmann, 1983). Twenty microliters of 5 mg/ml MTT (Sigma, USA) was added to each well and the plate was incubated at 37ºC for 3 h. Then MTT solution was removed, 100 µl DMSO was added and the absorbance of each well was measured with a microplate reader (BMG LabTech, Germany) at 570 nm. The dose (EC_{50} and EC_{100}) of the tested compounds was estimated by the Graphpad Instat software at 50% and 100% cell viability, respectively [1].

Human breast cancer cell lines:

Anticancer effect of the above-mentioned compounds was assayed using human breast cancer cell lines (MDA-MB 231 and MCF7) that were cultured in DMEM (Lonza, USA) supplemented with 10% FBS. All cancer cells (5x10^{3} cells/well) were seeded in sterile 96-well plates. After 24h, serial concentrations of the tested compounds were incubated with three cancer cell lines for 72 h at 37ºC in 5% CO_2 incubator. MTT method was done as described above. The half maximal inhibitory concentration (IC_{50}) values were calculated using the

Graphpad Instat software. Furthermore, cellular morphological changes before and after treatment with the most effective and safest anticancer compounds were investigated using phase contrast inverted microscope with a digital camera (Olympus, Japan) [1].

3.2. Flow cytometric analysis of apoptosis-mediated anticancer effect

The most effective compounds which exhibited the highest anticancer effect on both breast cell lines, were selected to investigate their proapoptotic effect following the incubation for 72 h with cells at 0.1 µg/ml. After trypsinization, the untreated and treated cancer cells were incubated with fluorescein isothiocyanate (FITC)-annexin V and propidium iodide (PI) for 15 min, in dark. After washing with PBS, the apoptotic cells were quantified using flow cytometry at FITC signal detector (FL1) against the phycoerythrin emission signal detector (FL2) for PI-stained necrotic cells and analyzed with FloMax software.

3.3. Caspase 3/7 activation assay

The caspase 3/7 activation was quantified in the untreated and the most active compounds-treated Caco-2 using Apo-ONE ® caspase 3/7 kit following the manufacturer's instructions. This kit used a non-fluorescence substrate that was cleaved by caspases resulting in the generation of the fluorescence signal of Rhodamine 110. This signal was measured by the fluorescence omega microplate reader (BMG LabTech, Germany) at 490 nm excitation and 520 nm emission [2].

3.4. Quantitative detection for the change in the expression of p21 and Bcl-2 genes in the treated cancer cells

Total RNAs of untreated and the most effective anticancer compounds-treated breast cancer cells were extracted using Gene JET RNA Purification Kit (Thermo Scientific, USA). The cDNA was synthesized from mRNA using cDNA Synthesis Kit (Thermo Scientific, USA). Real time PCR was performed using SYBR green master mix and specific primers (Forward/Reverse) were 5′-ATGTTTTGCCAACTGGCCAAG-3′/5′-TGAGCAGCGCTCATGGTG-3′, 5′-TCCGATCAGGAAGGCTAGAGTT-3′/5′-TCGGTCTCCTAAAAGCAGGC-3′, and 5′-TCCGATCAGGAAGGCTAGAGTT-3′/5′-TCGGTCTCCTAAAAGCAGGC-3′ for p53, BAX, and Bcl-2 genes, respectively. The $2^{-\Delta\Delta CT}$ equation was used to estimate the change in gene expressions in the treated cancer cells relative to untreated cancer cells [3-5].

3.5. Docking simulations

Docking was conducted employing Molecular Operating Environment (MOE) software package version MOE 2019.102, Chemical Computing Group, Montreal, Canada. The XIAP BIR2 domain coordinates bound to the reference inhibitor were downloaded from the protein databank (PDB ID: 4KJU Coordinates for MDM2

[6] was downloaded from RCSB PDB (PDB ID: 5LAW [7] Unwanted residues and solvent molecules were eliminated, then the crystal structure was prepared and refined employing the default "Structure preparation" MOE setting. The studied compounds were built *in silico* and energy minimized employing Amber10: EHT force field with reaction-field electrostatics (an interior dielectric constant of 1 and an exterior dielectric of 80) using an 8–10 Å cutoff distance. Docking simulations were conducted applying the Triangular matcher algorithm and Alpha HB as placement and scoring functions. The number of placements poses passed to the refinement step were set as 100 generating the top 5 non-redundant poses of the lowest binding energy conformers. Results were recorded as S-scores with RMSD value < 2Å. Graphical representations of the molecular interactions were generated and inspected.

3.5. Statistical analysis

The data are expressed as mean ± standard error of mean (SEM) and the significant values were considered at $p < 0.05$. One-way analysis of variance (ANOVA) was done by Tukey's test used for evaluating the difference between the mean values of the studied treatments. The analysis was done for three measurements using SPSS software version 16 [8].

4-- References

1 Mosdam, T. Rapid colorimetric assay for cellular growth and survival: application to proliferation and cytotoxic assay. J. Immunol. Methods **1983**, 65, 55-63.

2 Lakshmi, P.J.; Kumar, B.S.; Nayana, R.S.; Mohan, M.S.; Bolligarla, R.; Das, S.K.; Bhanu, M.U.; Kondapi, A.K.; Ravikumar, M. Design, synthesis, and discovery of novel non-peptide inhibitor of Caspase-3 using ligand based and structure based virtual screening approach. Bioorganic & medicinal chemistry **2009**, 17, 6040-6047.

3 Zilfou, J.T.; Lowe, S.W. Tumor suppressive functions of p53. Cold Spring Harbor perspectives in biology **2009**, 1, a001883.

4 Fulda, S.; Galluzzi, L.; Kroemer, G. Targeting mitochondria for cancer therapy. Nature reviews Drug discovery **2010**, 9, 447-464.

5 Salakou, S.; Kardamakis, D.; Tsamandas, A.C.; Zolota, V.; Apostolakis, E.; Tzelepi, V.; Papathanasopoulos, P.; Bonikos, D.S.; Papapetropoulos, T.; Petsas, T. Increased Bax/Bcl-2 ratio up-regulates caspase-3 and increases apoptosis in the thymus of patients with myasthenia gravis. In vivo **2007**, 21, 123-132.

6 R.F. Kester, A.F. Donnell, Y. Lou, S.W. Remiszewski, L.J. Lombardo, S. Chen, N.T. Le, J. Lo, J.A. Moliterni, X. Han J. Med. Chem., 56 (2013), pp. 7788-7803].

7 Andreas Gollner, Dorothea Rudolph, Heribert Arnhof, Markus Bauer, SophiaM. Blake, Guido Boehmelt, XiaoLing Cockroft, Georg Dahmann, Peter Ettmayer, Thomas Gerstberger, Jale KarolyiOezguer, Dirk Kessler, Christiane

8 Kofink, Juergen Ramharter, Jörg Rinnenthal, Alexander Savchenko, Renate Schnitzer, Harald Weinstabl, Ulrike Weyer-Czernilofsky, Tobias Wunberg, Darryl B. McConnell J. Med. Chem., 59 (22) (2016), pp. 10147-10162